Phase diagram of the Pluronic L64–H_2O micellar system from mechanical spectroscopy

Xuemao Zhou, Xuebang Wu,* Huaguang Wang, Changsong Liu,* and Zhengang Zhu
Key Laboratory of Materials Physics, Institute of Solid State Physics, Chinese Academy of Sciences, P.O. Box 1129, Hefei, Anhui, P.R. China, 230031
(Received 19 December 2010; published 7 April 2011)

The linear viscoelastic properties of aqueous Pluronic L64 solutions have been investigated at high copolymer concentrations (25–62 wt%) using our modified low-frequency mechanical spectroscopy. The concentration-temperature phase diagram of the L64/H_2O system was constructed by studying the evolution of the loss modulus and loss tangent as temperature is increased at a fixed frequency. A particular attention was focused on the dynamics approaching the beginning and ending points (39% and 60%) of the fusiform gel region in the phase diagram. The dynamics is found to have a similar viscoelastic behavior at the low and high concentrations, where a frequency scaling expected for a static percolated network is exhibited. Moreover, with increasing temperature, the system above the critical gel concentration undergoes a transition from a viscoelastic liquid to a solid gel through a percolated particle network. Therefore, our results suggest that the formation of the gel is dominated by the percolation of the particle clusters.

DOI: 10.1103/PhysRevE.83.041801 PACS number(s): 83.80.Uv, 83.80.Qr, 83.85.Vb, 83.60.Bc

I. INRODUCTION

Block copolymers are a class of soft materials that have attracted great interest in past years due to their applications in biotechnology, medical analysis, and drug systems [1]. Pluronics is a triblock copolymer system consisting of a central polypropylene oxide (PPO) block, with polyethylene oxide (PEO) blocks on either side. When in solution, the copolymer can exhibit very rich phase behavior and the phase diagrams have been obtained by static and dynamic light scattering [2–6], small angle neutron scattering (SANS) [4,5,7,8], small-angle x-ray scattering (SAXS) [9–11], nuclear magnetic resonance (NMR) spectroscopy [12], electron spin resonance [13], rheological measurement [4,7,9,11,14,15], and differential scanning calorimetry (DSC) [9,16].

At low temperatures, both PEO and PPO are hydrophilic, and so the PEO-PPO-PEO chains readily dissolve in water, existing as unimers. As the temperature increases, PPO tends to become less hydrophilic faster than PEO, and the copolymers acquire surfactant properties and aggregate to form micelles with the middle PPO block as the core and the PEO blocks as the corona. The conformation of the PPO blocks in spherical micelles depends on the hydrated water associated with the PEO blocks. The further increase of the temperature enlarges the spherical micelles to such an extent that the PPO blocks become stretched, resulting in a sphere-to-rod shape transition of micelles [11,17]. At higher concentrations and temperatures, the micelles can develop into gel and closely packed crystalline lattice structures.

Alexandridis *et al*. [12] studied the phase behavior of L64 in water using ^{2}H-NMR, polarizing microscopy, and ocular inspection. In the vicinity of 30 °C, the main phases detected with increasing polymer concentration are L_1 (micellar), H (hexagonal), L_α (lamellar), and L_2 (reverse micellar), respectively, as shown in Fig. 1. The fusiform gel region with hexagonal crystalline structure was found to be surrounded by the micellar solution; however, no detailed information about the criticality of the system near the gelation was provided, which is the subject of the present study. On the other hand, Chen *et al*. [18–20] studied the phase behavior of L64/D_2O system by SANS and photocorrelation measurements and realized many of the predictions of mode-coupling theory concerning the reentrant glass transition (Fig. 1). They suggested the gelation is related to the presence of long-living clusters, while the glass transition is due to crowding of particles. The SANS and simulation results of the F127/D_2O system suggest that the sol-gel transition is dominated by the formation of a percolated polymer network [21], while some researchers argue that the physical gelation is beyond percolation [22]. Thus there is a need to fully investigate the phase diagram of the copolymer close to gelation using different methods to get a better insight into the nature of physical gelation.

Previous mechanical studies of PEO-PPO-PEO solutions have shown that the sol-gel transition occurs when the copolymer concentration is above a critical value [23,24]. In this work, to examine the dynamic process close to gelation, we reported a detailed L64/H_2O phase diagram in the concentrated region using mechanical spectroscopy. We perform temperature sweep and frequency response experiments over a wide range of copolymer concentrations. We show that the dynamics of the L64/H_2O system exhibits a similar viscoelastic behavior approaching the beginning and ending points of the fusiform gel region, where a frequency scaling expected for a static percolated network is observed. Above the critical gel concentration, the system experiences transitions between liquidlike, percolation-like, and gel-like behaviors as the temperature is increased. Our results suggest that the formation of the gel arises from a percolated network.

II. EXPERIMENT

The Pluronic L64 ($PEO_{13}PPO_{30}PEO_{13}$) with a nominal molecular weight of 2900 and PEO content of 40 wt% is obtained from Sigma-Aldrich. Wu *et al*. [25] obtained for this copolymer a number-average molecular weight (M_n) of 3400 g/mol using vapor pressure osmometry, and a

*xbwu@issp.ac.cn; csliu@issp.ac.cn

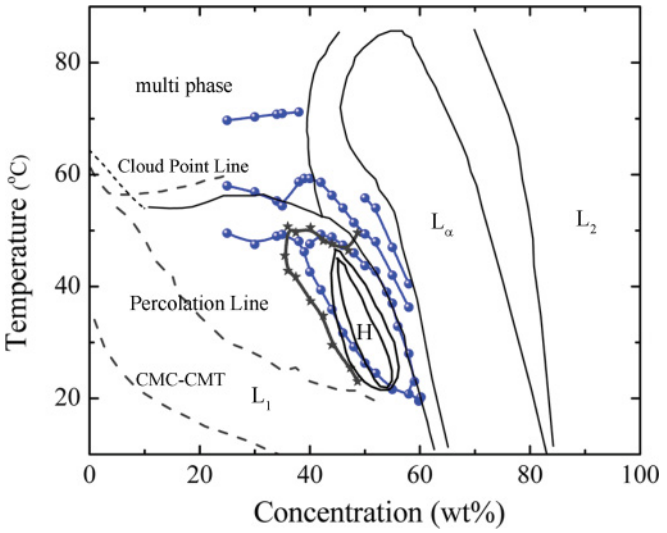

FIG. 1. (Color online) Temperature-concentration phase diagram of the L64/H_2O system solution deduced by mechanical spectroscopy (blue circles). The phase boundaries (solid lines) of one- and two-phase regions are indicated (redrawn from Ref. [12]), where L_1 is the micellar phase, H is the hexagonal phase, L_α is the lamellar phase, and L_2 is the reverse micellar phases. The CMT-CMC line, percolation line, cloud point line, and glassy line (pentagram symbols) were redrawn form Ref. [4].

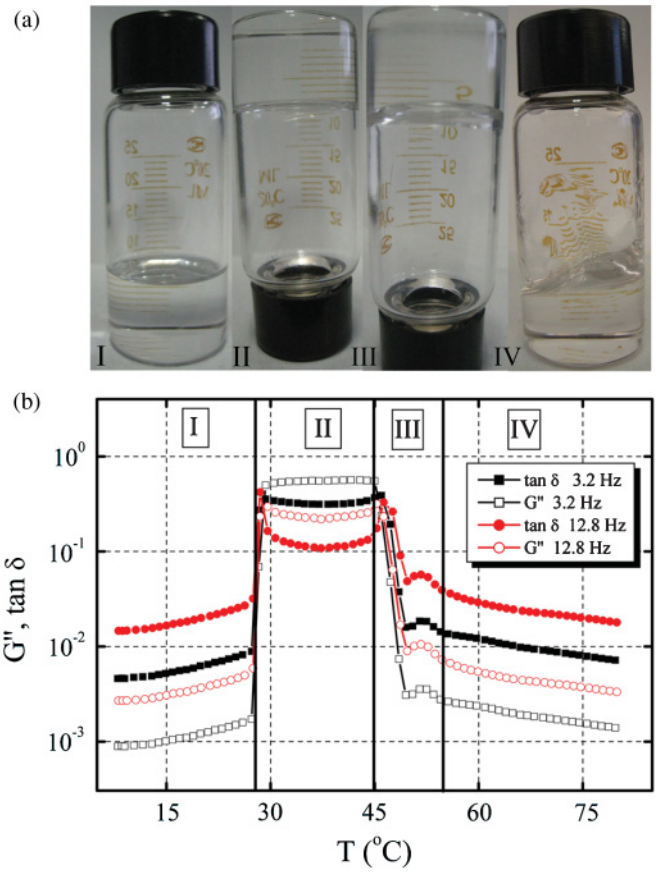

FIG. 2. (Color online) (a) Four patterns of 48% aqueous L64 solution with increasing temperature: (I) transparent liquid; (II) transparent gel; (III) turbid gel; and (IV) extremely viscous liquid. (b) Change in G'' (open symbols) and tanδ (full symbols) as a function of temperature for 48% aqueous L64 solution at 3.2 Hz (black squares) and 12.8 Hz (red circles). The corresponding (I), (II), (III), and (IV) regions were also indicated.

weight-average molecular weight (M_w) of 3700 g/mol from static light scattering measurements, thus yielding $M_w/M_n = 1.1$, an indication of low polydispersity. The solutions investigated in these studies were prepared from the same polymer lot number to minimize sample-to-sample variation. We chose to investigated the properties of the raw product (i.e., without further purification) as this is the form most likely to be used in application, and the method pursued by the majority of previously published characterization studies.

Concentrated aqueous solutions of the PEO-PPO-PEO copolymer with concentration (ϕ) of 25–62% (in wt%) were prepared by dissolving the copolymer in deionized water under stirring for 2 hours and then kept at 10 °C for seven days before being used. Measurements of the linear viscoelastic properties of L64 aqueous solutions were performed on our internally built torsion apparatus. The greatest advantage of our apparatus is capable of precisely measuring both the dilute complex fluids and the large viscous and concentrated ones in the frequency range of 10^{-3}–10^2 Hz. The sample was held between two stainless-steel bell-like cups. The inner cup was immersed in the aqueous solution, and the outer cup was surrounded by a water bath that controlled the temperature within 0.1 °C. The details of the device can be found elsewhere [26]. In the measurements, the inner cup is forced into torsional vibration by a time-dependent force $F(t) = F_0 \sin(\omega t)$, where ω is the circular frequency ($= 2\pi f$, f is the measuring frequency). The angular displacement function of the cup $A(t)$ is measured optically. In the case here, the response of the argument can be expressed as $A(t) = A_0 \sin(\omega t - \delta)$, where δ is the phase difference between $F(t)$ and $A(t)$. The loss tangent (tanδ) and the relative modulus ($G = G' + iG''$) were measured as functions of temperature or frequency.

The nonisothermal measurements were carried out with a heating rate of 0.3 °C/min to ensure the quasistatic test in a temperature range of 10–80 °C. The frequencies chosen were 0.05, 0.2, 0.8, 3.2, and 12.8 Hz, respectively. In the isothermal measurement, the measurements were performed in a frequency range of 0.02 to 12 Hz. In addition, the samples sealed in the graduated serum bottles were also examined by ocular inspection to check for sample homogeneity and mobility in the heating process. The homogeneity of the samples can be checked with the help of the graduation mark.

III. RESULTS AND DISCUSSION

To prove the sensitivity and validity of the apparatus, the phase transitions of L64/H_2O systems were investigated in a broad concentration and temperature range, and the experimental phase diagram is shown in Fig. 1. The fusiform gel region and the lamellar phase at high concentrations and temperatures were also observed. Overall, our data are consistent with those by other researchers [12,18], although there is a slight difference which may be due to the different heating rates in the measurements. Furthermore, we could

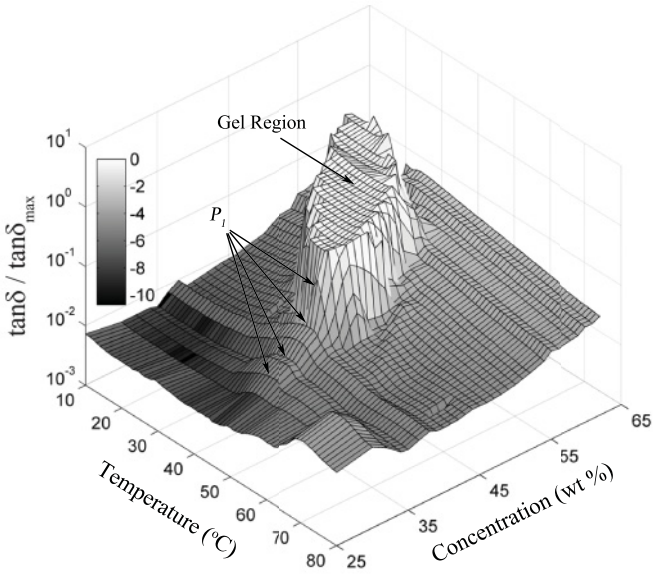

FIG. 3. The three-dimensional surface graph of the normalized loss tangent ($\tan\delta/\tan\delta_{max}$) in the concentration and temperature ranges of 25–62% and 10–80 °C at 3.2 Hz. Arrows indicate the small peaks of $\tan\delta$ (labeled as P_1) in the low temperature side for L64 aqueous solutions below 40%. The colormap parameter $C = (\tan\delta - \tan\delta_{min})/(\tan\delta_{max} - \tan\delta_{min})$ and the color change from white to dark indicates the decrease of ($\tan\delta/\tan\delta_{max}$). The gel region (white and upper) was seen from the magnitude of normalized loss tangent.

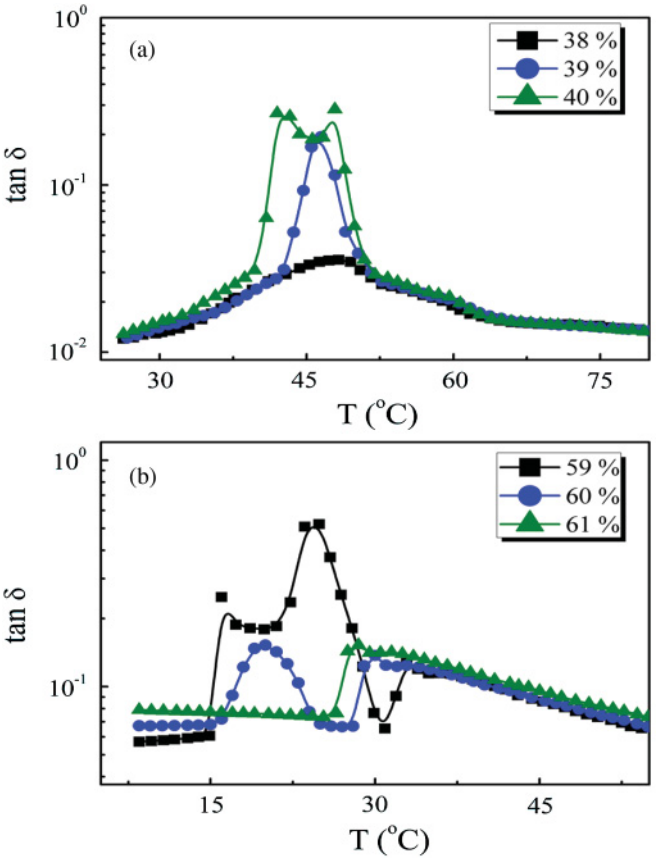

FIG. 4. (Color online) Mechanical loss spectra of L64 aqueous solution as a function of temperature at 12.8 Hz, where (a) $\phi = 38\%$ (black squares), 39% (blue circles), and 40% (olive triangles), and (b) $\phi = 59\%$ (black squares), 60% (blue circles) and 61% (olive triangles).

show the dynamic processes near the gel region and the existence of structural change in the multi phase.

Figure 2 shows the temperature dependence of loss modulus (G'') and loss tangent ($\tan\delta$) of 48 wt% L64 aqueous solution at $f = 3.2$ and 12.8 Hz. In comparison with the results from ocular inspection, as the temperature increases, the polymer solution is a transparent solution, transparent gel, turbid gel, and viscous solution in regions I, II, III, and IV, respectively. Note that both G'' and $\tan\delta$ describe the energy dissipation behaviors of materials and so they exhibit a similar behavior in the whole temperature range. As temperature increases up to 28 °C, a sharp increase in G'' and $\tan\delta$ indicates the occurrence of gelation. When the temperature reaches 45 °C, an abrupt drop in G'' and $\tan\delta$ implies the breakup of the gel structure. The appearance of G'' and $\tan\delta$ peaks at 52 °C indicates the formation of the lamellar phase in the high temperature side (Fig. 1). It should be noted that G'' and $\tan\delta$ do not depend on the frequencies, suggesting the mixture undergoes structural transitions rather than dynamic relaxations [23].

The variation of the normalized loss tangent ($\tan\delta$ / $\tan\delta_{max}$) versus temperature and concentration for the L64 aqueous solutions is plotted in Fig. 3. The fusiform gel region is seen from the magnitude of normalized loss tangent. The critical gel concentration of L64 aqueous solution is about 40%. At $\phi < 40\%$, $\tan\delta$ exhibits a small broad peak (P_1) in the low temperature side. As the concentration increases, the magnitude of the P_1 peak increases. The peak temperatures of different concentrations were reported in the phase diagram shown in Fig. 1. The mechanism of the P_1 peak is not clear at present. It is reasonable to suggest that the P_1 peak corresponds to the percolation transition of the micellar solution, although the resultant transition line is above the percolation line. Herein the data are deduced from the maximum of the peak whereas the percolation line from Chen *et al*. is deduced from the first increase step growth of the viscosity [18,19]. It is known that the mechanical loss of the liquid is proportional to the viscosity in some respect [27]. Thus for a fixed concentration, the transition temperature is above that deduced from the first increase of the viscosity. An additional indication comes from the analysis of the frequency dependence of the rheological quantities.

To investigate the criticality of the system near the gelation, we consider the results of mechanical loss spectra of L64 aqueous solutions at $\phi = 38$, 39, and 40%, and at $\phi = 59$, 60, and 61%, as shown in Fig. 4. At $\phi = 38\%$, with increasing temperature, the percolating phenomenon in this triblock copolymer micellar solution occurs. There is no tendency toward gelation since the micellar volume fraction is decreased due to the deformation of the spherical micelles. As ϕ is increased up to 39%, besides the P_1 peak, $\tan\delta$ exhibits an additional high peak superposed onto the P_1 peak. The second abrupt growth and immediately following sharp drop of $\tan\delta$ corresponds to the sol-gel transition and the gel-sol transition, respectively. The sol-gel transition occurs when the micellar volume fraction is above a critical value for

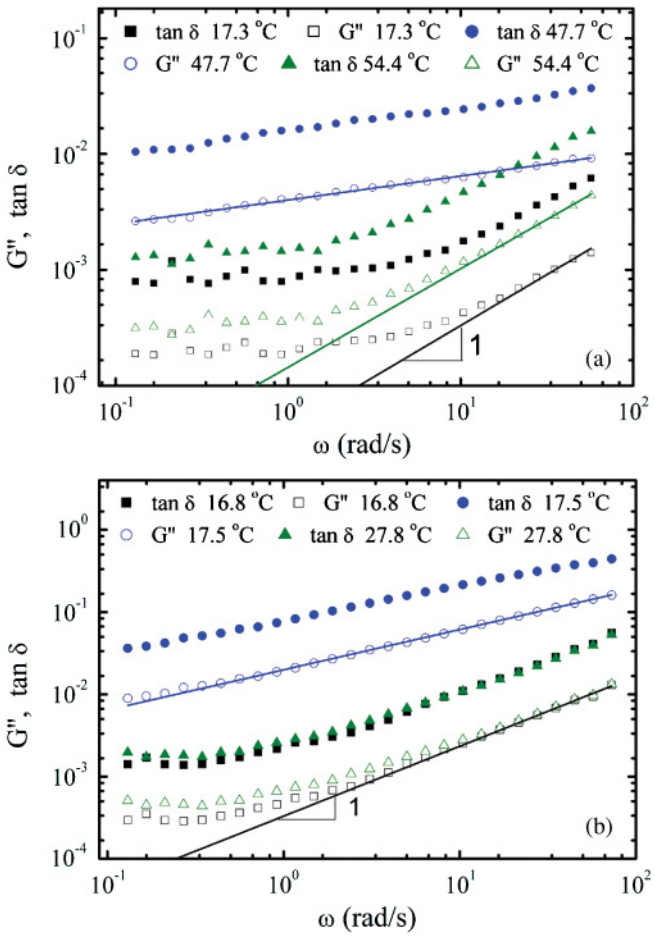

FIG. 5. (Color online) Frequency dependences of G'' (open symbols) and tanδ (full symbols) for (a) 38% and (b) 59.8% aqueous L64 solution as a function of temperature. At low and high temperatures, the lines show the low-frequency behavior of a viscoelastic liquid, while at the immediate temperatures, the blue (dark gray) lines show the frequency scaling expected for a static percolated network.

hard-sphere interaction [8,28]. As temperature increases, the percolating network of spherical micelles aggregates into a gel structure. The further increase of temperature reduces the micellar volume fraction, leading to the breakup of the gel. A similar result was observed by Mallamace *et al.*, [19] who considered the second growth as the structural arrest of the attractive glass transition. As the concentration reaches 40%, the enlarged micellar volume fraction can keep a high value at a broad temperature region, leading to the formation of a gel region. As can be observed in Fig. 4(b), the loss tangent behavior of L64 micellar solution near the gelation at the higher concentrations is very similar to that in the lower concentrations. As ϕ increases up to 60%, the spherical micelle deforms at low temperatures due to the increasing volume fraction of the hydrophobic domain, leading the gel to collapse [12].

To have a definitive confirmation on the percolation transition in the micellar system under study, we consider frequency dependence of its rheological quantities. In Fig. 5, the loss modulus G'' and loss tangent tanδ of 38% L64

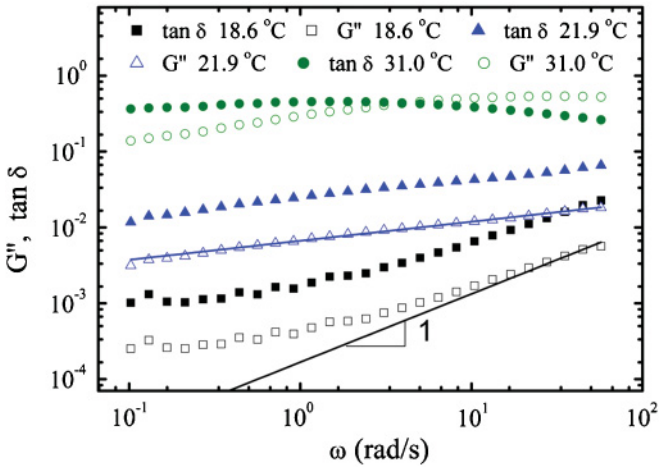

FIG. 6. (Color online) Frequency dependencies of G'' (open symbols) and tanδ (full symbols) for 54% aqueous L64 solution at temperatures: 18.6 °C (black squares), 21.9 °C (blue triangles), and 31.0 °C (olive circles). The mixture experiences transitions between liquidlike, percolation-like, and gel-like behaviors as the temperature is increased.

aqueous solution are plotted as a function of frequency, in a log-log scale. Figure 5(a) shows the spectra at three different temperatures (17.3, 47.7, and 54.4 °C). It can be seen that the system shows completely distinct behaviors. At low and high temperatures (17.3 and 54.4 °C), the frequency dependence of G'' approach the terminal behavior of a viscoelastic liquid, $G'' \sim \omega^1$, reflecting the liquidlike nature of the sample [29,30]. For $T = 47.7$ °C, G'' is characterized by a precise scaling behavior that can be ascribed to the percolation transition [4,31]. A similar result was observed for 59.8% L64 aqueous solution, where at 16.8 and 27.8 °C, the system exhibits liquidlike behavior while the percolation transition occurs at the immediate temperature $T = 17.5$ °C, as shown in Fig. 5(b). The theory of percolation applied to complex fluids (polymers, colloids, gels, etc.) predicts a universal scaling behavior [32]. At the percolation transition, G' and G'' have the following power-law dependence on frequency ω [4,31,33]

$$G' \sim G'' \sim \omega^n, \tag{1}$$

where n is an exponent used to describe viscoelasticity singularities near the percolation transition [4]. For 59.8% aqueous solution, the power-law fit of G'' yield the value $n = 0.4 \pm 0.005$, which is in good agreement with the values observed in some other gel-forming systems [33]. The percolation theory calculations presented by Muthukumar [34,35] suggest that the scaling exponent n is related to a fractal dimension d_f by

$$n = \frac{d(d+2-2d_f)}{2(d+2-d_f)}, \tag{2}$$

where d is the spatial dimension (and is equal to 3 here) and d_f relates the molecular weight of the polymeric aggregate M to its spatial size R by $R(d_f) \sim M$. In this case, solving yields $d_f = 2.1$, approaching the value of 2.5 predicted for percolation clusters at threshold [36] and comparable to values observed in other gels [33,37]. The recent diffusing wave spectroscopy (DWS) based microviscoelastic measurements do not

detect this scaling behavior expected for a static percolated network at low frequencies [38]. This should be due to the distinct differences between the microrheological and macrorheological characterization techniques, where the microrheology is dominated by local L64 micelle dynamics and not the bulk mechanical properties by macrorheological measurement.

Figure 6 shows the frequency dependence of G'' and tanδ of 54% L64 aqueous solution at three different temperatures (18.6, 21.9, and 31.0 °C). Similarly, at low temperature (18.6 °C), the system shows a frequency dependence of a viscoelastic liquid, and at $T = 21.9$ °C, a precise scaling behavior of G'' in ω is observed, corresponding to the percolation transition. For $T = 31.0$ °C, the viscoelasticity of the system changes dramatically. G'' exhibits a gradual increase with increasing f while tanδ shows an f-independent plateau, which is a characteristic of transient particle network [29,39]. In particular, gels characterized by short-range attractive potentials exhibit G' with a well-defined plateau [40], while gels characterized by high filler volume fractions and long-range attraction display marked relaxation dynamics [41]. In this last case, it has been suggested that gelation results from the crowding of clusters of weakly sticking particles. Herein, since the micelles form stable aggregates with a short-range interparticle attractive interaction [20], we speculate that the formation of the gel is dominated by the formation of a percolated particle cluster, which is consistent with the view by SANS and simulation [21]. Mallamace *et al.* [19] also suggested that the structural arrest, usually combining many features of gelation and glass transition [42], is related to the formation of a spanning cluster made of localized particles connected by bonds. Here we do not observe a marked minimum of G'' that is a hallmark of glasslike systems. In analogy with hard sphere glasses, the slow rearrangement in a glass of clusters would result in the weak frequency dependence of the viscoelastic properties, just as we observed experimentally for the gels [29].

IV. CONCLUSION

We have performed a systematic study of the phase behavior and dynamics of aqueous solutions of the triblock copolymer L64, using our modified low-frequency mechanical spectroscopy as the main experimental tool. To examine the dynamics approaching the beginning and ending points of the gel region, the temperature sweep and frequency response experiments close to gelation were measured. It is found that the system at high concentrations has a similar frequency scaling viscoelasticity expected for a percolated network to that in low concentrations. Above the critical gel concentration, the system experiences transitions between liquidlike, percolation-like, and gel-like behaviors as the temperature is increased. It is suggested that the formation of the gel both at low concentration and at high concentration is solely dominated by the percolation of the particle clusters.

ACKNOWLEDGMENTS

This work was financially supported by National Natural Science Foundation of China (Grants No. 50803066, No. 10874182, and No. 11074253).

[1] I. W. Hamley, *The Physics of Block Copolymers* (Oxford University Press, Oxford, 1998).
[2] G. Wanka, H. Hoffmann, and W. Ulbricht, Colloid Polym. Sci. **268**, 101 (1990).
[3] W. Brown, K. Schillen, M. Almgren, S. Hvidt, and P. Bahadur, J. Phys. Chem. **95**, 1850 (1991).
[4] L. Lobry, N. Micali, F. Mallamace, C. Liao, and S. H. Chen, Phys. Rev. E **60**, 7076 (1999).
[5] M. Duval, G. Waton, and F. Schosseler, Langmuir **21**, 4904 (2005).
[6] C. Chaibundit, N. M. P. S. Ricardo, C. A. Muryn, M. B. Madec, S. G. Yeates, and C. Booth, J. Colloid Interface Sci. **351**, 190 (2010).
[7] R. K. Prudhomme, G. W. Wu, and D. K. Schneider, Langmuir **12**, 4651 (1996).
[8] K. Mortensen, J. Phys. Condens. Matter **8**, A103 (1996).
[9] M. J. Park and K. Char, Macromol. Rapid Comm. **23**, 688 (2002).
[10] H. Lindner, G. Scherf, and O. Glatter, Phys. Rev. E **67**, 061402 (2003).
[11] V. Castelletto, P. Parras, I. W. Hamley, P. Baverback, J. S. Pedersen, and P. Panine, Langmuir **23**, 6896 (2007).
[12] P. Alexandridis, D. L. Zhou, and A. Khan, Langmuir **12**, 2690 (1996).
[13] A. Caragheorgheopol and S. Schlick, Macromolecules **31**, 7736 (1998).
[14] W. Brown, K. Schillen, and S. Hvidt, J. Phys. Chem. **96**, 6038 (1992).
[15] P. H. Mohan and R. Bandyopadhyay, Phys. Rev. E **77**, 041803 (2008).
[16] P. Alexandridis and J. F. Holzwarth, Langmuir **13**, 6074 (1997).
[17] R. Ganguly, N. Choudhury, V. K. Aswal, and P. A. Hassan, J. Phys. Chem. B **113**, 668 (2009).
[18] W. R. Chen, Y. Liu, F. Mallamace, P. Thiyagarajan, and S. H. Chen, J. Phys. Condens. Matter **16**, S4951 (2004).
[19] F. Mallamace, S. H. Chen, A. Coniglio, L. de Arcangelis, E. Del Gado, and A. Fierro, Phys. Rev. E **73**, 020402(R) (2006).
[20] S. H. Chen, W. R. Chen, and F. Mallamace, Science **300**, 619 (2003).
[21] Y. Q. Li, T. F. Shi, Z. Y. Sun, L. J. An, and Q. R. Huang, J. Phys. Chem. B **110**, 26424 (2006).
[22] S. K. Kumar and J. F. Douglas, Phys. Rev. Lett. **87**, 188301 (2001).
[23] X. B. Wu, Z. G. Zhu, S. Y. Shang, Q. L. Xu, J. P. Shui, and G. Z. Zhang, J. Phys. Condens. Matter **19**, 466102 (2007).
[24] X. B. Wu, Z. G. Zhu, Q. L. Xu, J. P. Shui, and G. Z. Zhang, Physica B **403**, 2500 (2008).
[25] G. Wu, Z. Zhou, and B. Chu, Macromolecules **26**, 2117 (1993).
[26] X. B. Wu, Q. L. Xu, J. P. Shui, and Z. G. Zhu, Rev. Sci. Instrum. **79**, 126105 (2008).

[27] G. Chen, Z. G. Zhu, and J. P. Shui, Acta Phys. Sin. **48**, 421 (1999).
[28] K. Mortensen, W. Brown, and B. Norden, Phys. Rev. Lett. **68**, 2340 (1992).
[29] G. Romeo, A. Fernandez-Nieves, H. M. Wyss, D. Acierno, and D. A. Weitz, Adv. Mater. **22**, 3441 (2010).
[30] K. Hyun, J. G. Nam, M. Wilhelm, K. H. Ahn, and S. J. Lee, Rheol. Acta **45**, 239 (2006).
[31] F. Mallamace, M. Broccio, P. Tartaglia, W. R. Chen, A. Faraone, and S. H. Chen, Physica A **330**, 206 (2003).
[32] D. Stauffer, *Introduction to Percolation Theory* (Taylor and Francis, London, 1985).
[33] J. P. Celli, B. S. Turner, N. H. Afdhal, R. H. Ewoldt, G. H. McKinley, R. Bansil, and S. Erramilli, Biomacromolecules **8**, 1580 (2007).
[34] M. Muthukumar, J. Chem. Phys. **83**, 3161 (1985).
[35] M. Muthukumar, Macromolecules **22**, 4656 (1989).
[36] D. Stauffer, A. Coniglio, and M. Adam, Adv. Polym. Sci. **44**, 103 (1982).
[37] K. S. Hossain, K. Miyanaga, H. Maeda, and N. Nemoto, Biomacromolecules **2**, 442 (2001).
[38] C. J. Kloxin and J. H. van Zanten, J. Chem. Phys. **131**, 134904 (2009).
[39] W. Wolthers, D. van den Ende, V. Breedveld, M. H. G. Duits, A. A. Potanin, R. H. W. Wientjes, and J. Mellema, Phys. Rev. E **56**, 5726 (1997).
[40] V. Trappe and D. A. Weitz, Phys. Rev. Lett. **85**, 449 (2000).
[41] V. Prasad, V. Trappe, A. D. Dinsmore, P. N. Segre, L. Cipelletti, and D. A. Weitz, Faraday Discuss. **123**, 1 (2003).
[42] A. Coniglio, L. De Arcangelis, E. Del Gado, A. Fierro, and N. Sator, J. Phys. Condens. Matter **16**, S4831 (2004).